J. Fluid Mech. (1983), *vol.* 126, *pp.* 413–430
Printed in Great Britain

Azimuthal rotation in the axisymmetric meridional flow due to an electric-current source

By V. BOJAREVIČS AND E. V. SHCHERBININ
Institute of Physics, Latvian S.S.R. Academy of Sciences, Salaspils, Riga 229021, U.S.S.R.

(Received 15 January 1982 and in revised form 20 July 1982)

The steady laminar flow driven by the meridional electromagnetic force due to an electric-current point source on a plane is considered. The previous studies of the problem (Shercliff 1970; Shilova & Shcherbinin 1971) lead to a self-similar solution of the full Navier–Stokes equations analogous to the classic Landau jet. The solution breaks down when a critical electric-current magnitude is exceeded (Sozou 1971). In the present paper the converging meridional flow is shown to be unstable to an axisymmetric azimuthal perturbation when the corresponding critical Reynolds number is exceeded. The flow solution breakdown is eliminated for the coupled converging and rotating flow. The physical process is suggested by the draining-vortex formation. The fluid-flow equations are solved by the Galerkin method, using expansions in Gegenbauer functions. The mechanism sustaining the rotation is examined; the increased angular momentum in the fluid region is maintained by the balance of viscous diffusion upstream and convection to the axis of symmetry. The experimental evidence for vortex formation is considered.

1. Introduction

In the last decade some authors have studied the problem of an electrically conducting fluid flow due to an electric-current point source since this is a convenient model for the investigation of some high-current industrial processes (electrical arcs, electro-slag welding, etc.) and natural phenomena (lightning discharge in a conducting fluid, tornado). The fluid motion in these processes is driven by the rotational Lorentz force set up by a diverging current and its associated magnetic field. The problem appeared in the papers of Zhigulev (1960), Lundquist (1969), Shercliff (1970), Sozou (1971) and Shilova & Shcherbinin (1971).

Further interest in the problem can be motivated by the fact that the fluid flow due to an electric-current source is described by a class of exact solutions of the Navier–Stokes equations. The class was introduced by Landau (1944), Yatseyev (1950) and Squire (1951). These solutions correspond to the axisymmetric meridional flows with velocity fields inversely proportional to a spherical radius. Goldshtik (1960) added an azimuthal velocity and considered the potential vortex viscous flow above a rigid plane. Wu (1961) extended the class of exact solutions to magnetohydrodynamics with the meridional magnetic field inversely proportional to a spherical radius. A full formulation of the class of exact solutions in magnetohydrodynamics was given by Shcherbinin (1969).

The solution obtained by Lundquist (1969) describes in the Stokes approximation the slow fluid flow due to an electric-current source on a plane. The flow converges along the plane and ascends along the axis of symmetry. A similar meridional flow is induced by a vortex line normal to a rigid plane (Goldshtik 1960). Goldshtik's

solution of the nonlinear problem shows that the axial velocity grows to infinity as the vortex line intensity approaches the finite value $\Gamma(0) = 8\nu$, where the parameter $\Gamma(0)$ is defined by $v_\phi = \Gamma(\theta)/r\sin\theta$. A similar singularity has been found by Sozou (1971) in the flow induced by an electric-current source. A numerical solution of the nonlinear equation governing the fluid flow leads to infinite axial velocity when a non-dimensional parameter $S = \mu_0 I^2/4\pi^2\rho\nu^2$, reaches the value $S_c \approx 150$. Here I is the magnitude of the total supplied electric current, μ_0 the magnetic permeability, ρ the density, and ν the kinematic viscosity. Narain & Uberoi (1971) extended the problem for an arbitrary conical rigid boundary and showed that the values of S_c increase as the cone angle θ_0 is decreased. So, for the case $\theta_0 = 90°$ (plane), $S_c \approx 150$, but, for $\theta_0 = 30°$, $S_c \approx 1200$.

Different viewpoints were expressed regarding the unlimited growth of velocities in the flow generated by an electric-current point source. Shercliff (1970) suggested that the fluid vorticity generated by rotational electromagnetic forces can be limited by viscous effects and by effects of flow-induced secondary electric currents. However, this balance cannot be achieved in an inviscid fluid model adopted by the author. Sozou & English (1972) dealt with a viscous-fluid model incorporating magnetic-field convection and found the same non-regularity of the solution at $S = S_c$ if the fluid conductivity was finite.

Sozou & Pickering (1976) attempted to improve the situation by restricting the fluid flow to a hemispherical container and abandoning the self-similar form of the solution. The numerical solution showed that the velocity grew faster than linearly with the parameter S; the maximum growth occurred on the axis of symmetry near the spherical boundary. The numerical results indicated a singularity of the axial velocity when a critical value of S was achieved. This value was even smaller than S_c of the corresponding infinite-domain problem.

Recently Atthey (1980) gave a numerical solution of the nonlinear problem of fluid flow in a hemispherical container due to the discharge from a finite electric-current source. The analysis of the results shows the velocity-field intensity growing slower than linearly with S. This is true except in the axial region near the spherical boundary where the axial velocity increases in much the same manner as in the case considered by Sozou & Pickering, yet at much greater magnitude of the parameter S ($\sim 10^5$). Thus difficulties remain computing velocity fields at large magnitudes of an electric current diverging from a small source.

In a review paper Moffatt (1978) concludes that the proposed solutions to the point-source problem contain internal inconsistencies that have yet to be fully resolved. Moffatt shows also that the mechanical work done in unit time by a rotational electromagnetic force can be limited only by viscous effects in a closed container.

Bojarevičs (1981*a*, *b*) has considered the same problem where an electric current I_2 is supplied to the point source by an isolated wire immersed in fluid along the axis of symmetry (figure 1). This situation models an immersed electrode in electro-slag welding when electric current flows to an axially symmetric lateral surface. In this case the flow direction is reversed. The flow diverging along the plane can be described by the class of exact solutions at practically any magnitude of the parameter S. The fluid flow is like an inviscid flow for $S = 10^6$–10^9, except in the narrow viscous layers at the plane and at the current-supplying wire. The flow is described analytically with the use of matched asymptotic expansions for $S \to \infty$.

These results give rise to a question: why is the flow direction crucial for the

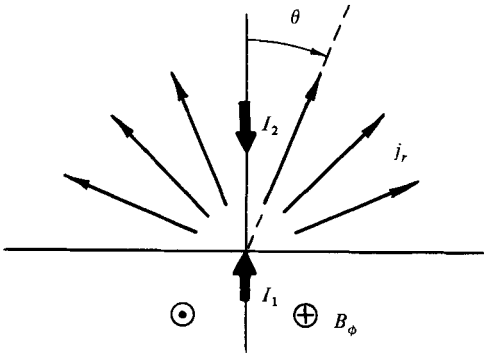

FIGURE 1. The electric current discharge from a point source on a plane $\theta = \frac{1}{2}\pi$. The total current $I = I_1$ is supplied from the outside of fluid, or $I = I_2$ is supplied along an isolated wire on $\theta = 0$.

solution? In the present paper it will be shown that the converging flow is unstable to an azimuthal disturbance, and that it can exist only when coupled with azimuthal rotation. This approach is suggested by the papers of Smislov & Shcherbinin (1976), Craine & Weatherill (1980) and Millere, Sharamkin & Shcherbinin (1980), where it is shown that the azimuthal rotation resulting from the application of an axial magnetic field can slow down the meridional flow or even reverse it. The new feature, reported in the paper of Millere *et al.* (1980), is the energy transfer from the meridional flow to the azimuthal rotation. This allows us to propose that a small azimuthal perturbation will be amplified by the intensive converging meridional flow in analogy with a draining-vortex formation.

The theoretical consideration is motived by experiment (Bojarevičs, Millere & Chaikovsky 1981); electric current is supplied to a small water-cooled electrode, 0·8 cm in diameter, in the centre of a free surface of mercury filling a hemispherical copper containiner, 36 cm in diameter, which serves as another electrode (see the photographs in figure 2). When the electric current $I = I_1$ is applied from above to the free surface, a converging flow is set up which closely resembles a flow drained to a sink. The observed flow for $I_1 \gtrsim 15$ A is coupled with rotation similar to a draining vortex (figure 2*a*). There are no sufficient external azimuthal forces to drive the rotation in this axially symmetric situation, but a small forced perturbation can be produced through interaction of the radial electric current and the vertical component of the Earth's magnetic field or the field of distant non-symmetric parts of the current-supplying wires. This perturbation field is about 0·5 G in magnitude, compared with the magnitude of maximum self-magnetic field, 500 G, for 1000 A input current. Rotation is not observed in the reversed flow when the electric current $I = I_2$ is supplied from below to the free surface (figure 2*b*), and even after artificial spin-up, the rotation soon dies out and there remains only the diverging radial flow along the free surface.

The following theoretical analysis does not concern a perturbation growth in time or space, but involves sharp changes in a stationary flow increasing the Reynolds number R_s (defined in §2). A perturbation is introduced in the form of a small stationary force $\mathbf{f}_0$, which provokes sharp velocity-field changes in the vicinity of the critical R_s value. Moreover, the case $\mathbf{f}_0 = 0$ differs essentially from the result obtained by decreasing the finite value $\mathbf{f}_0 \to 0$. This new solution includes an azimuthal rotational motion sustained by the converging meridional flow. A viscous mechanism

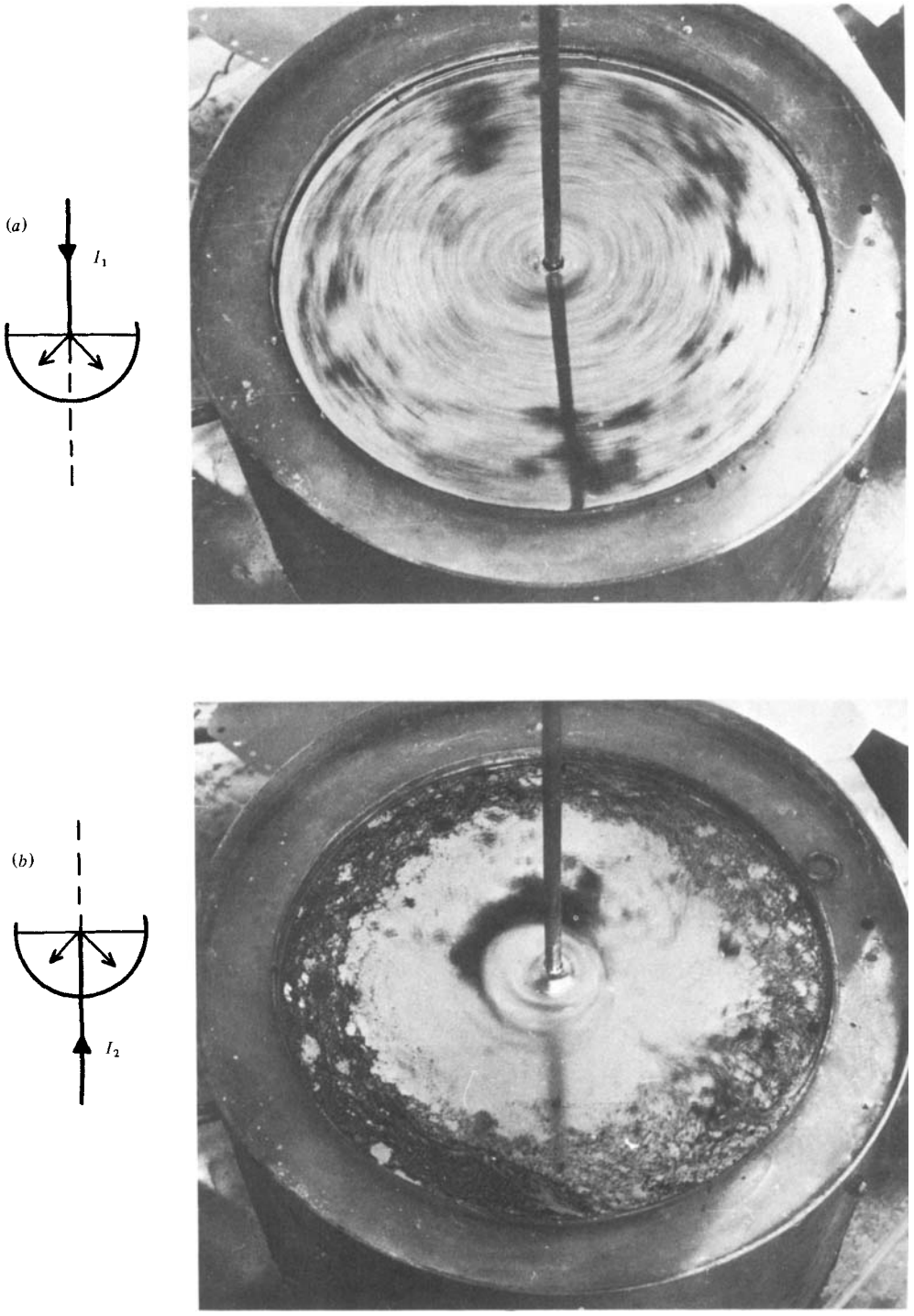

FIGURE 2. Flow on the surface of mercury in a hemispherical container. (*a*) If electric current $I_1 = 1200$ A is supplied from above, converging flow is coupled with rotation. (*b*) If electric current $I_2 = 1200$ A is supplied from below, diverging flow does not rotate. The surface is deformed in the centre, where fluid ascends.

supporting the intensive rotation is analysed in §5. A basic feature of the mechanism is an upstream viscous diffusion of the angular momentum. In §6 we discuss the relevance of the semi-infinite flow to a real bounded flow.

2. Formulation of the problem

The stationary motion of a viscous incompressible electrically conducting fluid is governed by the Navier–Stokes equations, which, after eliminating the pressure, take the form

$$-\rho\nabla\times(\mathbf{v}\times\nabla\times\mathbf{v}) = -\nu\rho\nabla\times\nabla\times\nabla\times\mathbf{v}+\nabla\times(\mathbf{j}\times\mathbf{B}), \tag{1}$$

$$\nabla.\mathbf{v} = 0. \tag{2}$$

For small magnetic Reynolds number the magnetic field is approximately independent of fluid motion. Then a steady magnetic field $\mathbf{B}$ and an electric current density $\mathbf{j}$ in the fluid must satisfy the following equations:

$$\nabla\times\mathbf{j} = 0, \tag{3}$$

$$\nabla\times\mathbf{B} = \mu_0\mathbf{j}, \tag{4}$$

$$\nabla.\mathbf{j} = 0, \tag{5}$$

$$\nabla.\mathbf{B} = 0. \tag{6}$$

The radial electric current from a point source in the origin of spherical polar co-ordinates (r, θ, ϕ) is given by the equation

$$\mathbf{j} = \left(-\frac{1}{r^2}L'(\mu), 0, 0\right), \tag{7}$$

where a prime denotes the differentiation with respect to the variable $\mu = \cos\theta$. From (3) it follows that

$$L(\mu) = I(A\mu+B). \tag{8}$$

To specify the constants A, B consider the situation where a half-space $\theta \leqslant \frac{1}{2}\pi$ is occupied by a conducting fluid. Then the constants in (8) differ in two cases: (i) if the electric current $I = I_1$ is supplied to the source along a line wire on $\theta = \pi$, then $A = -1/2\pi$, $B = 1/2\pi$; (ii) if the electric current $I = I_2$ is supplied along an isolated line wire immersed in the fluid on $\theta = 0$, then $A = -1/2\pi$, $B = 0$.

The electromagnetic force resulting from the electric current's self-magnetic field $B_\phi = \mu_0 L(\mu)/r(1-\mu^2)^{\frac{1}{2}}$ contains only a θ-component,

$$\mathbf{f}_e = \mathbf{j}\times\mathbf{B} = \mu_0\frac{LL'}{r^3(1-\mu^2)^{\frac{1}{2}}}\mathbf{e}_\theta, \tag{9}$$

and drives a fluid flow either converging to the axis of symmetry ($f_{e\theta} < 0$) (in case (i)), or diverging ($f_{e\theta} > 0$) (in case (ii)).

From dimensional analysis (Shcherbinin 1969; Sozou 1971) the velocity field

$$\mathbf{v} = \left(-\frac{1}{r^2}\frac{\partial\psi}{\partial\mu}, -\frac{1}{r(1-\mu^2)^{\frac{1}{2}}}\frac{\partial\psi}{\partial r}, v_\phi\right) \tag{10}$$

is self-similar, and the stream function ψ and the azimuthal velocity v_ϕ take the forms

$$\psi = rI\left(\frac{\mu_0}{\rho}\right)^{\frac{1}{2}}g(\mu), \quad v_\phi = \frac{I}{r}\left(\frac{\mu_0}{\rho}\right)^{\frac{1}{2}}\frac{\Omega(\mu)}{(1-\mu^2)^{\frac{1}{2}}}. \tag{11}$$

The previous investigations have shown two different flow situations: (i) the converging-flow solution exhibits a breakdown if the total supplied current I exceeds a certain critical value (Sozou 1971); (ii) the diverging flow smoothly evolves with increasing I, and develops thin viscous boundary layers separated by an inviscid flow region when $I \to \infty$ (Bojarevičs 1981*a*, *b*).

In the converging flow a small azimuthal disturbance may be amplified by the inviscid mechanism of vortex-line stretching (see Batchelor 1967, §5.2). For the purpose of investigating flow sensitivity to azimuthal disturbances, let us introduce a small azimuthal volume force, $\mathbf{f}_0 = f_{0\phi}\,\mathbf{e}_\phi$, in such a way as to conserve the self-similar fluid-flow situation. Then a magnetic-field disturbance suitable for the experimental situation can be modelled in the class of exact solutions by an external field

$$\mathbf{B}_0 = \frac{k\mu_0 I}{r}\left(C, \frac{1}{(1-\mu^2)^{\frac{1}{2}}}(C\mu + D), 0\right), \tag{12}$$

where k is a small constant proportional to the perturbation. We specify further $C = -1$, $D = 1$, so that the magnetic-force lines are parabolas in a meridional plane with apexes on the axis $\theta = \pi$ outside the fluid. Interaction of the magnetic field $\mathbf{B}_0$ (12) and the radial electric current (7) gives the disturbing azimuthal force

$$f_{0\phi} = j_r B_{0\theta} = \frac{k\mu_0 I^2}{r^3}(-A)\frac{C\mu + D}{(1-\mu^2)^{\frac{1}{2}}}. \tag{13}$$

Note that (13) is the same for the cases (i) $I = I_1$ or (ii) $I = I_2$.

Inserting (11), (A 9) and (A 10) (see appendix A) in the fluid-flow equations (A 7) and (A 8), after some manipulations we get a system of ordinary differential equations:

$$\tfrac{1}{2}(1-\mu^2)(g^2)''' + 2\Omega\Omega' = \frac{1}{R_s}(1-\mu^2)(2g'' + ((1-\mu^2)g'')'') + 2A(A\mu + B), \tag{14}$$

$$g\Omega' = \frac{1}{R_s}(1-\mu^2)\Omega'' - kA(C\mu + D), \tag{15}$$

where the Reynolds number R_s is defined by

$$R_s = I\left(\frac{\mu_0}{\rho}\right)^{\frac{1}{2}}\Big/\nu = 2\pi S^{\frac{1}{2}}.$$

We assume that the plane $\theta = \frac{1}{2}\pi$ is a free non-deformed fluid surface. This is not a realistic assumption for the high-current experimental situation shown in figure 2, but it is a good approximation for the moderate-R_s flows actually considered here. Then boundary conditions for the viscous fluid-flow equations are

$$g(0) = g''(0) = \Omega'(0) = 0 \quad \text{on the surface} \quad \mu = 0, \tag{16}$$

$$g(1) = \Omega(1) = (1-\mu^2)^{\frac{1}{2}}g''(1) = 0 \quad \text{on the axis} \quad \mu = 1. \tag{17}$$

3. The numerical method

The solution of the boundary-value problem (14)–(17) is characterized by large changes in the functions $g(\mu, R_s)$ and $\Omega(\mu, R_s)$ in the vicinity of the critical R_s value. This imposes special requirements to approximation accuracy of a numerical solution. We have used a variant of the Galerkin method which has an advantage in accuracy over finite-difference methods (Orszag 1971). This method can also be easily extended to non-self-similar problems involving spherical boundaries.

We assume that the functions $g(\mu)$ and $\Omega(\mu)$ can be expanded in converging series of the form:

$$g = \sum_{n=1}^{\infty} a_{2n+1} \mathscr{I}_{2n+1}(\mu), \tag{18}$$

$$\Omega = \sum_{n=1}^{\infty} b_{2n} \mathscr{I}_{2n}(\mu), \tag{19}$$

where $\mathscr{I}_n(\mu)$ are the orthonormal Gegenbauer functions of the first kind of order n and of power $-\frac{1}{2}$. The functions $\mathscr{I}_n(\mu)$ are the operator-E^2 (see appendix A) eigenfunctions appearing in slow-flow linearized problems. $\mathscr{I}_n$ are closely related to the Legendre functions $P_n(\mu)$: $\mathscr{I}_n = (P_{n-2} - P_n)/(2n-1)$; for properties of $\mathscr{I}_n$ see Happel & Brenner (1965). The expansions in Gegenbauer functions have been successfully used by Dennis & Singh (1978) to compute flow variables for the case of rotating spheres.

$\mathscr{I}_n(\mu)$ are even or odd functions of μ according as n is even or odd. Therefore, choosing odd functions in the expansion (18) and even in (19), we have fulfilled all the boundary conditions (16), (17). The function $A\mu + B$ in (14) may be defined as an antisymmetric function for $\mu < 0$, and $C\mu + D$ in (15) as a symmetric function for $\mu < 0$. Then employing the orthogonality properties

$$\int_{-1}^{1} \frac{\mathscr{I}_m \mathscr{I}_n}{1-\mu^2} d\mu = \begin{cases} 0 & (m \neq n), \\ 2/(2n+1) & (m = n) \end{cases} \tag{20}$$

for $m, n \geqslant 2$, these functions $A\mu + B$ and $C\mu + D$ can be expanded in the series of odd or even functions $\mathscr{I}_n(\mu)$ respectively.

To specify the coefficients a_{2n+1} and b_{2n}, we insert the expansions (18), (19) in the fluid-flow equations (14), (15). Then, multiplying (14) by $\mathscr{I}_{2l+1}$, (15) by $\mathscr{I}_{2l}$ and integrating in accordance with the orthogonality (20), we get a set of $2N$ nonlinear algebraic equations:

$$\sum_{m=1}^{N-1} \sum_{n=1}^{N-m} [a_{2n+1} a_{2m+1} (-2n(2n+1) M(2l, 2m, 2n) - (3 \cdot 2m(2m+1) + 2n(2n+1)) L(2l, 2m, 2n)) + b_{2n} b_{2m} 2L(2l, 2m-1, 2n-1)] = \frac{1}{R_s} a_{2l+1} \frac{(2l-1)(2l+2)}{4l+1} + \frac{1}{l(2l+1)} A(A + B - BP_{2l}(0)), \tag{21}$$

$$\sum_{m=1}^{N-1} \sum_{n=1}^{N-m} a_{2m+1} b_{2n} L(2l-1, 2m, 2n-1) = -\frac{1}{R_s} b_{2l} \frac{1}{4l-1} - \frac{1}{2l(2l-1)} kA(C + D - C\mathscr{I}_{2l}(0)), \tag{22}$$

where $l = 1, 2, \ldots, N$; N is a truncation number in the expansions (18), (19). In deriving (21), (22) there are assumed *a posteriori* the asymptotic relations for large n: $a_{2n+1} = O(b_{2n}) = o(a_{2n-1})$, and the terms $o(a_1 a_{2N+1})$ are not included in (21), (22). The integrals involving triple products of the Gegenbauer functions are evaluated after the manner of Dennis & Singh (1978). Our slightly different expressions for L and M are to be found in appendix B.

An iterative procedure is used to solve the set of equations (21), (22). At each iteration step the coefficients on the right-hand side of (21), (22) are determined using the most recently available information for the left-hand side. Each resulting solution member is denoted by $a_{2n+1}^{t+\frac{1}{2}}$ or $b_{2n}^{t+\frac{1}{2}}$, and the new approximation is defined:

$$a_{2n+1}^{t+1} = \Delta a_{2n+1}^{t+\frac{1}{2}} + (1-\Delta) a_{2n+1}^{t}, \quad 0 < \Delta \leqslant 1, \tag{23}$$

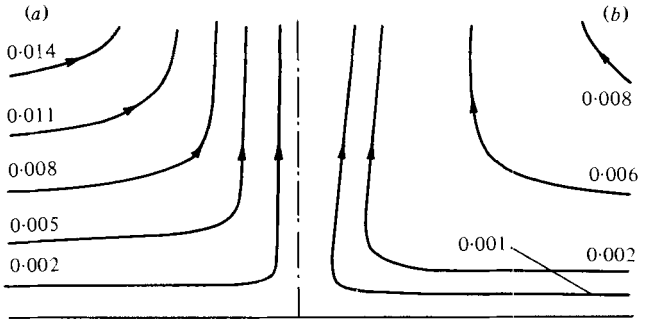

FIGURE 3. Meridional streamlines rg/R_s = const: (*a*) Non-rotating flow: $k = 0$, $R_s = 42$. (*b*) Rotating flow: $k = 0{\cdot}01$, $R_s = 44$.

and analogously for b_{2n}. The value of Δ must be decreased when the iteration procedure tends to diverge as R_s number is increased towards its critical value.

The results described in §4 correspond to the truncation number $N = 20$ in the expansions (18), (19). Moreover, the numerical results differ by less than 1 % if $N = 15$ for $R_s \leqslant 200$ and $k = 0{\cdot}01$. The test problems with $k = 0$ (without azimuthal rotation) show good agreement with the earlier works (Sozou 1971; Bojarevičs 1981*a*).

4. Results

A slow fluid motion, when inertia effects are negligible, is governed by the linear Stokes equations. The linear solution to the problem (14)–(17) can be easily constructed by equating the left-hand sides of (21), (22) to zero. In this case, the functions $g(\mu, R_s, k)$ and $\Omega(\mu, R_s, k)$ are determined independently, and $g \sim R_s$, $\Omega \sim kR_s$. We introduce the normalized functions

$$g_n = \frac{1}{R_s} g, \quad \Omega_n = \frac{1}{kR_s} \Omega \tag{24}$$

for the purpose of demonstrating a nonlinear evolution of the flow variables when the inertial effects are included.

Consider the nonlinear fluid-flow problem (14)–(17) in the case where the electric current $I = I_1$ is supplied along a wire from the external side of the fluid surface (figure 1). Neglecting an azimuthal fluid motion as in the earlier works, we insert $k = 0$ in (15) and assume the trivial solution $\Omega = 0$. Then increasing R_s we find that the axial velocity tends to infinity as $R_s \to R_c \approx 43$ (the curve (*a*) in figure 4). Streamlines of the flow in the vicinity of R_c are shown in figure 3(*a*).

Let us introduce the azimuthal perturbation (13). If we fix the small parameter k and increase R_s this corresponds to the case of a perturbation proportional to kI^2, e.g. the perturbation due to small spiralling asymmetry of the supplying wire. When the parameters k and R_s are small, the normalized axial velocity $g_n'(1)$, and azimuthal velocity on the free surface $\Omega_n(0)$ are constant (figures 4, 5). On increasing R_s, both meridional flow and azimuthal velocities grow (figures 4, 5). Increased centrifugal forces near the free surface, where $\Omega(\mu)$ is maximal, counteract the positive radial pressure gradient which corresponds to the converging flow along the plane $\theta = \frac{1}{2}\pi$. This leads to decreased meridional convection, and velocities at R_c remain finite. (Streamlines in the presence of the azimuthal perturbation are shown in figure 3(*b*).) Moreover, the normalized axial velocity $g_n'(1)$ attains a maximum

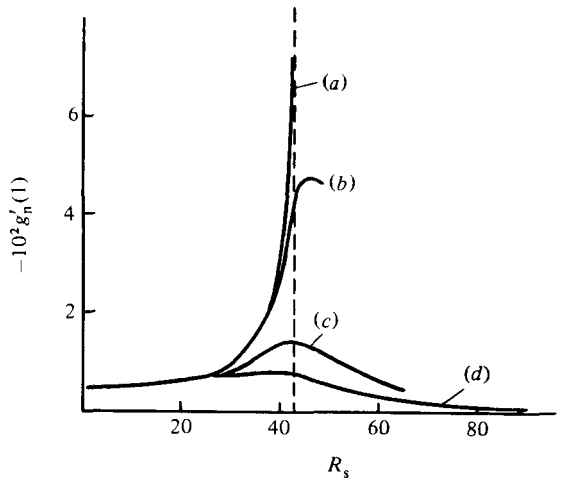

FIGURE 4. The axial-velocity dependence upon R_s: (*a*) $k = 0$; (*b*) 0·001; (*c*) 0·005; (*d*) 0·01.

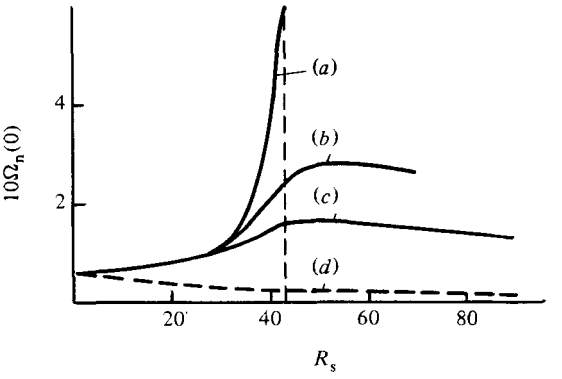

FIGURE 5. The dependence upon R_s of the azimuthal velocity on the free surface: (*a*) $k = 0{\cdot}001$; (*b*) 0·005; (*c*) 0·01; (*d*) 0·01 (diverging meridional flow for $I = I_2$).

and decreases further as R_s is increased (the curves (*b*)–(*d*) in figure 4). The normalized azimuthal velocity on the free surface $\Omega_n(0)$ varies in the same manner (the curves (*b*), (*c*) in figure 5).

The relative maximum magnitude of azimuthal velocity with increasing R_s is small when $k \approx 1$, and is not of particular note; this situation corresponds to the results of Smislov & Shcherbinin (1976), Craine & Weatherill (1980) and Millere *et al.* (1980). The numerical solution of the present problem shows that, on decreasing the perturbation parameter k, the maximum value of Ω_n increases rapidly in the vicinity of R_c (figure 5) and g_n' remains finite (figure 4). This result may be interpreted as the small azimuthal-motion perturbation is amplified by the intensive meridional flow. The question arises as to whether the function Ω_n would grow infinitely if $k \to 0$. Then an infinitesimal perturbation can be amplified to the level necessary for interaction with the meridional flow, thus limiting the axial velocity growth when $R_s \to R_c$. In figure 6 is plotted the inverse to $\Omega_n(0)$ if $k \to 0$ for various R_s. If $R_s < R_c$ the magnitude of $1/\Omega_n$ is finite at $k = 0$. But for $R_s \geqslant R_c$ the numerical results suggest that $1/\Omega_n \to 0$ as $k \to 0$.

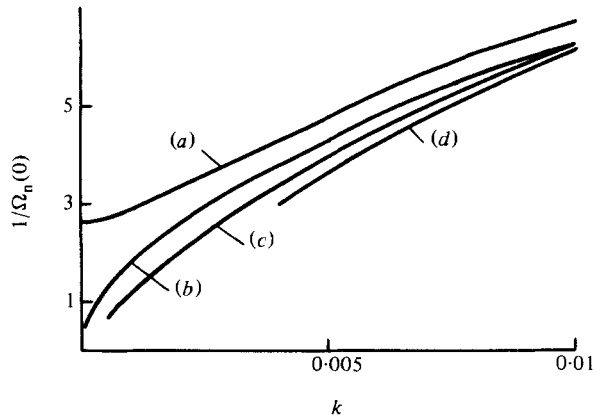

FIGURE 6. The inverse of the azimuthal velocity when the perturbation parameter $k \to 0$: (*a*) $R_s = 40$; (*b*) 42; (*c*) 45; (*d*) 50.

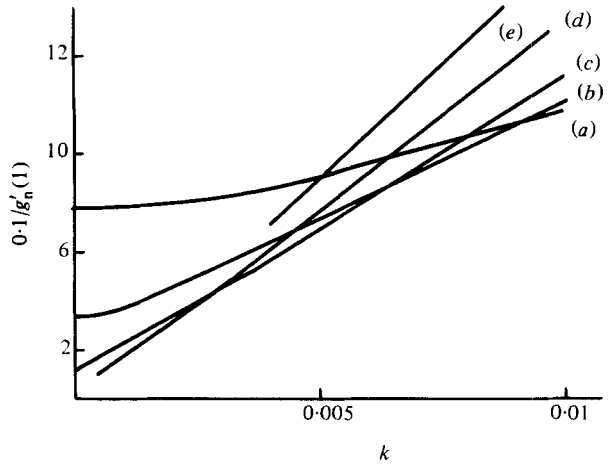

FIGURE 7. The inverse of the axial velocity when $k \to 0$: (*a*) $R_s = 35$; (*b*) 40; (*c*) 42; (*d*) 44; (*e*) 50.

Consider the limiting behaviour in more detail. At finite values of k the magnitude of $g_n'(1)$ remains bounded on increasing $R_s \geqslant R_c$ (figure 4), consequently the finite perturbation (13) eliminates the singularity of axial velocity. If we let k tend to zero along the solution induced by the azimuthal perturbation, the asymptotic behaviour of the numerical solution at R_c suggests that $\Omega_n \sim \text{const}/k$ (figure 6), and owing to (24) $\Omega \sim \text{const}$. From figure 7, representing the inverse of axial velocity, it can be deduced that $g_n'(1)$ may remain finite when $k \to 0$. Note that the curvature $\partial^2(1/g_n')/\partial k^2$ of the curves in figure 7 do not change sign on approaching R_c, unlike those of the curves in figure 6. The closest computed results to the limit $k = 0$ are represented in figure 8. But the limit $k = 0$ cannot be reached because then the angular momentum source in the symmetric flow is lost. When $k = 0$ (15) can be integrated:

$$\Omega' = \text{const} \times \exp \int_0^\mu \frac{R_s g}{1-t^2} dt, \tag{25}$$

and for the boundary conditions (16), (17) it follows that $\Omega \equiv 0$. Consequently, an

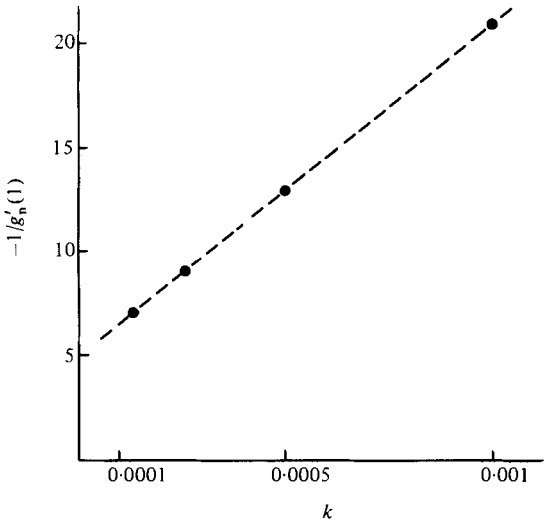

FIGURE 8. The inverse of the axial velocity when $k \to 0$ for $R_s = 43 \approx R_c$.

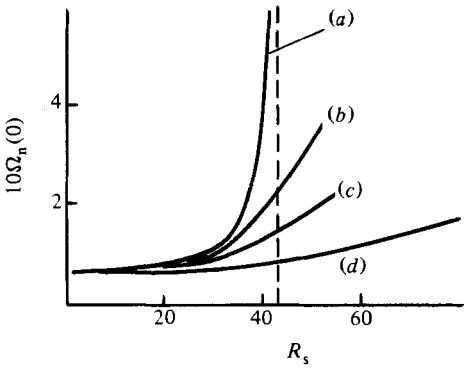

FIGURE 9. The azimuthal velocity on the free surface for fixed magnitude of the disturbing force (13): (*a*) $kR_s^2 = 1$; (*b*) 10; (*c*) 20; (*d*) 50.

infinitesimal but non-zero azimuthal perturbation is necessary to avoid a singularity in the axial velocity if $R_s \geqslant R_c$.

If we fix the magnitude of the perturbing force $f_{0\phi}$ (13), proportional to kR_s^2, then the behaviour of the calculated solution is analogous to the previous case with k fixed. The normalized azimuthal velocity increases in proportion to R_s when $R_s > R_c$ (figure 9). If we let $f_{0\phi} \to 0$, then $1/\Omega_n \to 0$ at $R_s \geqslant R_c$, analogously with the previous case.

The increase of the velocity of rotation, $\sim \Omega_n$, is associated with converging flow. The flow that diverges along the free surface, generated by supplying the electric current $I = I_2$ along an immersed wire on $\theta = 0$, does not amplify the rotation (the dashed curve in figure 5). A small perturbation of the form (13) does not change the diverging meridional flow significantly.

5. The mechanism sustaining the rotation

A curious property of the converging flow described in §4 is that of acquiring a relatively large rotation velocity as the result of a small azimuthal disturbance. This feature is notable in such well-known phenomena as a draining vortex or tornadoes. The large rotation velocities in these phenomena are commonly associated with vortex-line stretching in a converging flow, but viscous diffusion is necessary to sustain the rotation without supplying angular momentum from the environment. The Burgers vortex is a model of the stretching–diffusion balance (see Batchelor 1967), although it does not satisfy the viscous boundary conditions.

The present solution of the fluid-flow equations can be used to analyse the mechanism sustaining the increased angular momentum in the converging flow due to an electric-current source. Consider the conservation of the angular momentum $m_z = \rho r \sin\theta v_\phi$ with respect to the symmetry axis $\theta = 0$. The use of the angular momentum instead of the appropriate vorticity component is justified by the physically simple integral conservation equation. The conservation equation can be derived from the vector product of the cylindrical radius vector $r_c \mathbf{e}_{rc}$ ($r_c = r\sin\theta$) and the azimuthal momentum equation. Using the divergent form of the momentum equations (Weir 1976), the scalar m_z conservation equation is

$$\rho \operatorname{div}(\mathbf{v} r\sin\theta v_\phi) = \nu\rho[\operatorname{div}\operatorname{grad}(r\sin\theta v_\phi) - 2\operatorname{div}(\mathbf{e}_{rc} v_\phi)] + r\sin\theta f_{0\phi}. \tag{26}$$

Integrating (26) over a control volume V with a surface S_0, we can use Gauss' theorem and write the equation in the form

$$\rho \oint_{S_0} r\sin\theta v_\phi \mathbf{v} \,.\, d\mathbf{S}_0 = \nu\rho \oint_{S_0} [\operatorname{grad}(r\sin\theta v_\phi) - 2v_\phi \mathbf{e}_{rc}] \,.\, d\mathbf{S}_0 + \int_V r\sin\theta f_{0\phi}\, dV, \tag{27}$$

which represents the balance of convection and diffusion of angular momentum across the surface S_0, and the modification due to electromagnetic forces.

The control volume V may be specified between the coordinate surfaces: $\theta = \theta_2 = \frac{1}{2}\pi$, $\theta = \theta_1 < \frac{1}{2}\pi$, $r = r_2$, $r = r_1 < r_2$. Inserting in (27) the definition of velocities (10), (11), (24), electromagnetic force (13), and accounting for the boundary conditions (16) (m_z is not carried across the free surface), the conservation equation can be written as

$$-R_s^2 \int_0^{\mu_1} g_n' \Omega_n \, d\mu + R_s^2 g_n(\mu_1)\Omega_n(\mu_1) = -2\int_0^{\mu_1} \Omega_n \, d\mu + [(1-\mu_1^2)\Omega_n'(\mu_1) + 2\mu_1 \Omega_n(\mu_1)] + A(\tfrac{1}{2}\mu_1^2 - \mu_1), \tag{28}$$

where $\mu = \cos\theta$, and all the terms are reduced by the factor $r_2 - r_1$ owing to the flow self-similarity. The terms in (28) represent the rate of change of angular momentum $m_z = I(\mu_0\rho)^{\frac{1}{2}}\Omega(\mu)$ in the control volume V. The first term of the left-hand side is proportional to the convective transfer of m_z out of the volume V across the surface $r = r_2$ (since r_1 can be chosen to be zero), the second term is proportional to that across the surface $\theta = \theta_1$. On the right-hand side the first term represents the diffusive transfer of m_z inside V across the surface $r = r_2$ (or the frictional torque on the outer side of $r = r_2$), the second term represents the transfer across the surface $\theta = \theta_1$. The third term represents the perturbation by the electromagnetic force $f_{0\phi}$.

Consider the angular momentum balance in fluid layers separated by surfaces

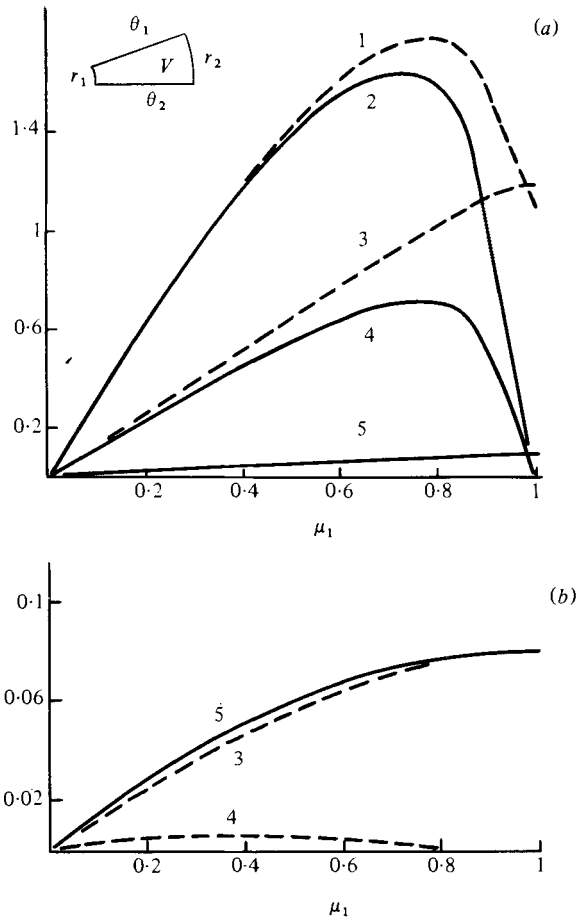

FIGURE 10. The angular-momentum conservation equation (28) terms *vs.* the variable control volume boundary $\mu_1 = \cos\theta_1$. The control volume is sketched in the upper corner. The curve number represents the term number from the left-hand side, negative-term values are shown with dashed lines. (*a*) $R_s = 43$, $k = 0{\cdot}001$; (*b*) 1, 0·001.

$\theta = \text{const}$. In figure 10 are plotted the magnitudes of terms in the conservation equation (28) as functions of the variable control-volume boundary μ_1. In the absence of strong meridional convection ($R_s = 1$) the electromagnetic force moment (the curve 5 in figure 10) is compensated by the negative frictional torque on the outer surfaces $r = r_2$ and $\theta = \theta_1$ (curves 3 and 4) or, in other words, by the diffusion of m_z from the volume V. The strong meridional convection directed to the axis of symmetry changes essentially the distribution of the terms in (28) to maintain the angular momentum balance. Figure 10(*a*) presents the magnitudes of terms in (28) for $R_s = 43 \approx R_c$. The electromagnetic force moment (curve 5), which has induced the azimuthal motion, is now much smaller in magnitude than the convectic angular momentum transfer in unit time through the surfaces $r = r_2$ (curve 1) and $\theta = \theta_1$ (curve 2). The viscous diffusion, also much greater in magnitude than the perturbation momentum, is directed against the converging meridional flow (curves 3 and 4). This also implies the positive torque acting on the outer surface $\theta = \theta_1$ of the volume V. Thus, the increased magnitude of the angular momentum m_z is sustained in the fluid

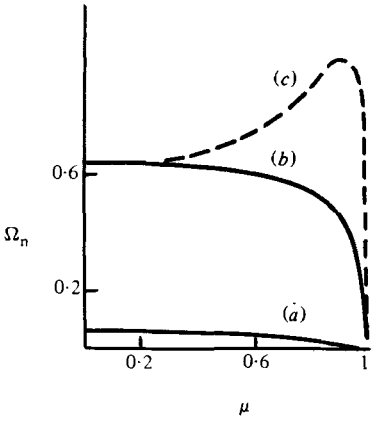

FIGURE 11. The normalized angular momentum $\Omega_n(\mu)$ and azimuthal velocity $\Omega_n(\mu)/(1-\mu^2)^{\frac{1}{2}}$ at fixed r (dashed line) for $k = 0{\cdot}001$: (*a*) $R_s = 1$ (both curves coincide in the scale of the figure); (*b*, *c*) = 43.

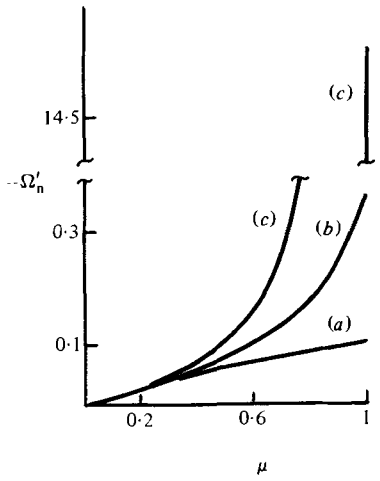

FIGURE 12. The radial vorticity component $\Omega_n'(\mu)$ for $k = 0{\cdot}001$: (*a*) $R_s = 1$; (*b*) 30; (*c*) 43.

volume, where the self-similar flow exists, by the double process of diffusion upstream and convection backwards. The increase in angular momentum may be interpreted as a result of momentum growth in time due to action of the diffusion–convection mechanism: the momentum expelled by diffusion is returned by convection and the perturbation is added in this process. Of course, there must exist another fluid region where the angular momentum is transferred, e.g. by the viscous friction to a rigid boundary. The corresponding flow in a closed rigid container is analysed by Bojarevičs & Millere (1982), and the similar mechanism sustaining increased angular momentum in an axial region is found.

There are also changes in the azimuthal velocity $v_\phi(\mu)$. For the case of the strong converging meridional flow ($R_s = 43$) the azimuthal velocity at a fixed radial distance r, $v_\phi \sim \Omega/(1-\mu^2)^{\frac{1}{2}}$, attains its maximum near the axis $\mu = 1$, and exceeds the magnitude on the free surface $\mu = 0$ (figure 11). In the slow flow ($R_s = 1$) the maximum azimuthal velocity is on the free surface (figure 11).

Vorticity components for the self-similar flow are of the form

$$\operatorname{curl}\mathbf{v} = I\left(\frac{\mu_0}{\rho}\right)^{\frac{1}{2}}\left(-\mathbf{e}_r\frac{1}{r^2}\Omega'(\mu),\ 0,\ \mathbf{e}_\phi\frac{(1-\mu^2)^{\frac{1}{2}}}{r^2}g''(\mu)\right). \tag{29}$$

In the absence of rotation the magnitude of vorticity grows infinitely near the axis of symmetry for $R_s \to R_c$, and the viscous diffusion in this case does not prevent the flow breakdown. The flow is unstable to an azimuthal perturbation; therefore the radial vorticity also attains a large magnitude near the axis of rotation (figure 12); but the increased viscous diffusion leads to limited vorticity growth.

6. Concluding remarks

There remains uncertainty as to whether the self-similar fluid-flow model may be related to a real bounded flow. An appropriate model for the investigation would be the fluid flow in a hemispherical container. Results of the computational study of the flow between concentric hemispherical electrodes are reported by Bojarevičs & Millere (1982). The results reveal the significance of the ratio r_1/r_2 of the inner to outer hemisphere radii; for the small ratio $r_1/r_2 \leqslant 0{\cdot}1$, there forms a region of the increased rotation near the inner sphere where increased angular momentum is sustained. The flow in this region tends to the self-similar flow if $r_1/r_2 \to 0$.

Other experimental evidence can be found for the transition to rotation in converging axisymmetric flows when a critical Reynolds number is exceeded. Kawakubo *et al.* (1978) report formation of a vortex in a sink flow when the sink intensity exceeds a certain value. Torrance (1979) reports an azimuthal rotation of the laboratory plume above a localized heat source, though with non-axisymmetric oscillations. Atmospheric vortices (tornadoes) are associated with convective flows, and some relation with the above process may be suggested in their formation stage.

Appendix A

In the axisymmetric situation the solenoidal stationary vector fields $\mathbf{v}, \mathbf{j}, \mathbf{B}$ can each be described by the use of two scalar functions:

$$\mathbf{v} = \left(\frac{1}{H_2H_3}\frac{\partial\psi}{\partial q_2},\ -\frac{1}{H_1H_3}\frac{\partial\psi}{\partial q_1},\ v_\phi\right), \tag{A 1}$$

$$\mathbf{j} = \left(\frac{1}{H_2H_3}\frac{\partial\psi_1}{\partial q_2},\ -\frac{1}{H_1H_3}\frac{\partial\psi_1}{\partial q_1},\ j_\phi\right), \tag{A 2}$$

$$\mathbf{B} = \left(\frac{1}{H_2H_3}\frac{\partial\psi_2}{\partial q_2},\ -\frac{1}{H_1H_3}\frac{\partial\psi_2}{\partial q_1},\ B_\phi\right), \tag{A 3}$$

where (q_1, q_2, ϕ) is an orthogonal axisymmetric coordinate system with Lame coefficients H_1, H_2, H_3. By the use of (4) the electric-current function ψ_1 is related to the azimuthal magnetic field B_ϕ induced by the meridional electric current:

$$\psi_1 = \frac{1}{\mu_0}H_3B_\phi + \text{const.} \tag{A 4}$$

From (3) it follows that ψ_1 must satisfy the equation

$$E^2\psi_1 \equiv \frac{H_3}{H_1H_2}\left(\frac{\partial}{\partial q_1}\frac{H_2}{H_1H_3}\frac{\partial}{\partial q_1}+\frac{\partial}{\partial q_2}\frac{H_1}{H_2H_3}\frac{\partial}{\partial q_2}\right)\psi_1 = 0. \tag{A 5}$$

The function ψ_2 characterizes an external magnetic field which is not associated with a current in the fluid. ψ_2 is governed by the equation

$$E^2\psi_2 = 0. \tag{A 6}$$

Substituting (A 1)–(A 3) in the fluid-flow equations (1), we express them in the curvilinear coordinates:

$$H_3(\nabla\psi\times(\nabla H_3^{-2}+H_3^{-2}\nabla)E^2\psi - H_3v_\phi\nabla H_3^{-2}\times\nabla(H_3v_\phi))\,.\,\mathbf{e}_\phi+\nu E^4\psi = -\frac{\mu_0}{\rho}H_3\psi_1(\nabla H_3^{-2}\times\nabla\psi_1)\,.\,\mathbf{e}_\phi, \tag{A 7}$$

$$\nabla\psi\times\nabla(H_3v_\phi)\,.\,\mathbf{e}_\phi+\nu H_3E^2H_3v_\phi = \frac{1}{\rho}(\nabla\psi_2\times\nabla\psi_1)\,.\,\mathbf{e}_\phi, \tag{A 8}$$

where

$$\nabla = \mathbf{e}_1H_1^{-1}\frac{\partial}{\partial q_1}+\mathbf{e}_2H_2^{-1}\frac{\partial}{\partial q_2};$$

$\mathbf{e}_1$, $\mathbf{e}_2$, $\mathbf{e}_3$ are the unit vectors of the coordinate system.

In the spherical polar coordinates (r,θ,ϕ) the Lame coefficients are $H_1=1$, $H_2=r$, $H_3=r\sin\theta$. The velocity field is given by (10); the electric current and the external magnetic field from §2 can be related to the functions

$$\psi_1 = L(\mu) = I(A\mu+B), \tag{A 9}$$

$$\psi_2 = -k\mu_0Ir(C\mu+D). \tag{A 10}$$

Appendix B

We define

$$L(l,m,n) = \frac{1}{2}\int_{-1}^{1}\frac{1}{1-\mu^2}\mathscr{I}_{l+1}\mathscr{I}_{m+1}\mathscr{I}'_{n+1}\,d\mu, \tag{B 1}$$

$$M(l,m,n) = \int_{-1}^{1}\frac{\mu}{(1-\mu^2)^2}\mathscr{I}_{l+1}\mathscr{I}_{m+1}\mathscr{I}_{n+1}\,d\mu. \tag{B 2}$$

By the use of associated Legendre functions of the first kind,

$$P_n^1(\mu) = n(n+1)\mathscr{I}_{n+1}(\mu)/(1-\mu^2)^{\frac{1}{2}},$$

and the relation $\mathscr{I}'_{n+1}(\mu) = -P_n(\mu)$, Gegenbauer functions can be related to spherical harmonics

$$Y_{lm}(\theta,\phi) = e^{im\phi}\left(\frac{2l+1}{4\pi}\frac{(l-m)!}{(l+m)!}\right)^{\frac{1}{2}}P_l^m(\cos\theta). \tag{B 3}$$

Spherical harmonics, their integrals and other related results are described by Varshalovich, Moskalev & Hersonsky (1975). The above integrals can be evaluated:

$$L(l,m,n) = \frac{n(n+1)-l(l+1)-m(m+1)}{2l(l+1)m(m+1)}\begin{pmatrix} l & m & n\\ 0 & 0 & 0\end{pmatrix}^2, \tag{B 4}$$

$$M(l,m,n) = -L(l,m,n)+\Lambda\begin{pmatrix} l & m & n\\ 0 & 0 & 0\end{pmatrix}^2, \tag{B 5}$$

where

$$\Lambda = \frac{l(l+1)[n(n+1)-l(l+1)+m(m+1)]+m(m+1)[n(n+1)+l(l+1)-m(m+1)]}{2l(l+1)m(m+1)n(n+1)}$$

and 3-j symbols $\begin{pmatrix} l & m & n \\ 0 & 0 & 0 \end{pmatrix}$ are equal to zero unless $|l-m| < n < l+m$. We compute them numerically by the use of recurrence relations and various symmetries which help to avoid error summation and ensure a test. All the necessary properties of the 3-j symbols can be found in Varshalovich *et al.*

REFERENCES

ATTHEY, D. R. 1980 A mathematical model for fluid flow in a weld pool at high currents. *J. Fluid Mech.* **98**, 787–801.

BATCHELOR, G. K. 1967 *An Introduction to Fluid Dynamics*. Cambridge University Press.

BOJAREVIČS, V. 1981*a* MHD flows due to an electric current point source. Part 1. *Magn. Gidrodin.* No. 1, 21–28.

BOJAREVIČS, V. 1981*b* MHD flows due to an electric current point source. Part 2. *Magn. Gidrodin.* No. 2, 41–44.

BOJAREVIČS, V. & MILLERE, R. 1982 Amplification of azimuthal rotation in meridional electrically induced vortical flow in a hemisphere. *Magn. Gidrodin.* To appear in No. 4.

BOJAREVIČS, V., MILLERE, R. & CHAIKOVSKY, A. I. 1981 Investigation of the azimuthal perturbation growth in the flow due to an electric current point source. In *Proc. 10th Riga Conf. on MHD*, Salaspils, vol. 1, pp. 147–148.

CRAINE, R. E. & WEATHERILL, N. P. 1980 Fluid flow in a hemispherical container induced by a distributed source of current and a superimposed uniform magnetic field. *J. Fluid Mech.* **99**, 1–12.

DENNIS, S. C. R. & SINGH, S. N. 1978 Calculation of the flow between two rotating spheres by the method of series truncation. *J. Comp. Phys.* **28**, 297–314.

GOLDSHTIK, M. A. 1960 A paradoxical solution of the Navier–Stokes equations. *Prikl. Mat. Mekh.* **24**, 610–621.

HAPPEL, J. & BRENNER, H. 1965 *Low Reynolds Number Hydrodynamics*. Prentice-Hall.

KAWAKUBO, T., TSUTCHIYA, Y., SUGAYA, M. & MATSUMURA, K. 1978 Formation of a vortex around a sink. *Phys. Lett.* **68** A, 65–66.

LANDAU, L. D. 1944 On a new exact solution of the Navier–Stokes equations. *Dokl. Akad. Nauk SSSR* **43**, 299–301.

LUNDQUIST, S. 1969 On the hydromagnetic viscous flow generated by a diverging electric current. *Ark. Fys.* **40**, 89–95.

MILLERE, R. P., SHARAMKIN, V. I. & SHCHERBININ, E. V. 1980 On the effect of longitudinal magnetic field on the electrovorticity flow in a cylindrical container. *Magn. Gidrodin.* No. 1, 81–85.

MOFFATT, H. K. 1978 Some problems in the magnetohydrodynamics of liquid metals. *Z. angew. Math. Mech.* **58**, T65–T71.

NARAIN, J. P. & UBEROI, M. S. 1971 Magnetohydrodynamics of conical flows. *Phys. Fluids* **14**, 2687–2692.

ORSZAG, S. 1971 Numerical simulations of incompressible flows within simple boundaries. 1. Galerkin (spectral) representation. *Stud. Appl. Math.* **50**, 293–327.

SHCHERBININ, E. V. 1969 On a class of exact solutions in the magnetohydrodynamics. *Magn. Gidrodin.* No. 4, 46–58.

SHERCLIFF, J. A. 1970 Fluid motion due to an electric current source. *J. Fluid Mech.* **40**, 241–250.

SHILOVA, E. I. & SHCHERBININ, E. V. 1971 MHD vortex flow in a cone. *Magn. Gidrodin.* No. 2, 33–38.

SMISLOV, Y. N. & SHCHERBININ, E. V. 1976 Nonlinear magnetohydrodynamic tornado model. In *Problems of Mathematical Physics* (ed. V. M. Tuchkevich), pp. 271–282. Nauka.

SOZOU, C. 1971 On the fluid motions induced by an electric current source. *J. Fluid Mech.* **46**, 25–32.

SOZOU, C. & ENGLISH, H. 1972 Fluid motions induced by an electric current discharge. *Proc. R. Soc. Lond.* A **329**, 71–81.

SOZOU, C. & PICKERING, W. H. 1976 Magnetohydrodynamic flow due to the discharge of an electric current in a hemispherical container. *J. Fluid Mech.* **73**, 641–650.

SQUIRE, H. B. 1951 The round laminar jet. *Q. J. Mech. Appl. Math.* **4**, 321–329.

TORRANCE, K. E. 1979 Natural convection in the thermally stratified enclosures with localized heating from below. *J. Fluid Mech.* **95**, 477–495.

VARSHALOVICH, D. A., MOSKALEV, A. N. & HERSONSKY, V. K. 1975 *The Quantum Theory of Angular Momentum.* Nauka.

WEIR, A. D. 1976 Axisymmetric convection in a rotating sphere. Part 1. *J. Fluid Mech.* **75**, 49–79.

WU, C.-S. 1961 A class of exact solutions of the magnetohydrodynamic Navier–Stokes equations. *Q. J. Mech. Appl. Math.* **14**, 1–19.

YATSEYEV, V. I. 1950 On a class of exact solutions of the viscous fluid flow equations. *Zh. Eksp. Teor. Fiz.* **20**, 1031–1034.

ZHIGULEV, V. N. 1960 On ejection effect due to an electrical discharge. *Dokl. Akad. Nauk SSSR* **130**, 280–283.